ELSEVIER

Physics of the Earth and Planetary Interiors 83 (1994) 283–297

PHYSICS OF THE EARTH AND PLANETARY INTERIORS

Application of the CMT algorithm to analog recordings of deep earthquakes

Wei-Chuang Huang *[,a], Göran Ekström [b], Emile A. Okal [a], Mikhail P. Salganik [b]

[a] *Department of Geological Sciences, Northwestern University, Evanston, IL 60208, USA*
[b] *Department of Earth and Planetary Sciences, Harvard University, Cambridge, MA 02138, USA*

Received 6 September 1993; revision accepted 30 January 1994

Abstract

The distribution and characteristics of deep earthquakes provide important information on both the large-scale aspects of mantle convection as well as on the small-scale mechanics of apparent shear failure within descending lithospheric plates at large confining pressures. Neither of these processes is well understood, but the detailed knowledge of the spatial and temporal distribution of earthquakes, as well as the focal geometries, scalar moments, and details of the earthquake rupture process, provides constraints which can be used to differentiate between competing models of mantle circulation and theories of deep seismic rupture. With the objective of expanding and improving the database of source parameters for deep earthquakes, we evaluate the feasibility of applying the Harvard centroid moment tensor (CMT) algorithm to earlier (pre-1977) earthquakes recorded on seismographs with analog recording. Abundant records from the World Wide Standardized Seismograph Network (WWSSN) are available for events after 1962, and the data from these high-quality stations with a known standard response are easily digitized and subjected to analysis by the CMT algorithm. For earlier events, no standardized network of seismometers is available. Using a modern deep earthquake as a test case, we show that reliable single-station moment tensor solutions can be obtained from the Press–Ewing instrument at Pasadena. We apply the single-station technique to three historical earthquakes recorded on different types of electromagnetic and mechanical seismographs: the 1957 Java earthquake (Press–Ewing); the 1922 Peru earthquake (Wiechert); and the 1911 Peru–Brazil earthquake (Galitzin). Robust results can be achieved from these data provided the instruments are well calibrated, and an analysis of selected earlier deep earthquakes may quickly double or triple the time span of the database of deep earthquake source parameters.

1. Introduction

The purpose of this paper is to explore the feasibility of extending the centroid moment tensor (CMT) algorithm (Dziewonski et al., 1983) to the analysis of analog records of historical earthquakes at the bottom of subduction zones ($h \geqslant 300$ km).

Even though deep earthquakes are a prime window on the process of subduction, and have provided great insight into physical conditions

* Corresponding author.

SSDI 0031-9201(94)02939-9

and processes inside slabs (e.g. recently, Creager and Jordan, 1984; Spakman et al., 1989; Zhou, 1990; Lundgren and Giardini, 1992), a number of problems remain outstanding, notably how apparent shear failure occurs at the relevant pressures (10–25 GPa) where ordinary brittle fracture is unlikely. A number of studies have invoked a depth- and temperature-dependent combination of brittle fracture and failure in ductile deformation, allowing the distribution of deep seismicity to be compared with the lithospheric strength predicted by laboratory studies of mineral strength (Griggs, 1972; Molnar et al., 1979; Wortel, 1986; Hobbs and Ord, 1988). In addition, over the past few years, a number of promising theories of deep seismic failure have been put forward that invoke phase changes during descent. One class of theories suggests that martensitic-like transformations might lead to macroscopic shear instability in such phase transformations as olivine → spinel (Meade and Jeanloz, 1989; Lomnitz-Adler, 1990). Another class suggests amorphization and dehydration of serpentine, extending the depth range of brittle failure through the support of normal stresses across fractures by fluid pressure (Raleigh, 1967; Meade and Jeanloz, 1991). Lastly, it has been proposed that deep seismicity could result from transformational faulting, a form of shear failure involving a low-pressure, low-density mineral phase (such as olivine) carried metastably into the field of a high-pressure, high-density one (such as spinel) (e.g. Burnley and Kirby, 1982; Burnley et al., 1991; Kirby et al., 1991). Present observations and our current insight into deep seismic failure are insufficient to establish definitively which, if any, of these competing theories are correct. However, transformational faulting for example, would predict a number of testable features in the exact location, size and energetics of seismicity at the bottom of subduction zones.

An additional question raised by deep earthquakes is that of their potential location at preferential sites along the Wadati–Benioff zones, and of the possible existence of repeat patterns; i.e., 'do large deep shocks have a tendency to recur at the same location at more or less regular intervals of time, in a way similar to the cycles often (but not always) described in the case of shallow interplate events?' The Harvard CMT catalog documents only one case of two earthquakes with $M_0 \geq 10^{26}$ dyn-cm occurring within a three-dimensional radius of 50 km of each other's centroid over its 16 year lifetime (the events of 22 October 1977 and 21 December 1983 in northern Argentina); furthermore, recent work on the 1921–1922 earthquakes in northern Peru indicates that they are significantly smaller than, and distant from, the nearby 1970 Colombian shock, despite larger assigned magnitudes (Okal and Bina, 1994). It is clear that progress towards answering any of the above questions requires a firm knowledge of the principal parameters of the seismicity of deep subducted slabs.

The most homogeneous and complete dataset of deep earthquakes is the Harvard CMT catalog (Dziewonski et al., 1981; Dziewonski and Woodhouse, 1983, subsequent updates published quarterly in Physics of the Earth and Planetary Interiors), which has become a standard tool for many aspects of geophysical research. One of the limitations of this catalog is its relatively short time span; it currently contains data for world seismicity only since 1977. This period is clearly too short to cover properly the 'earthquake cycle', believed to be of the order of several decades to centuries for interplate earthquakes, and possibly much longer for intraplate events. Indeed, since 1970 the seismic activity in nearly all depth ranges has been unusually weak, and any conclusions on the level of maximum seismicity as a function of depth inferred from the CMT dataset would be significantly biased by its short time span, especially for depths greater than 500 km. This is best demonstrated by the fact that the catalog contains 774 earthquakes below 300 km, whose cumulative moment (1.9×10^{28} dyn-cm) remains less than that of a single of their predecessors—the 1970 Colombian earthquake.

A few seismic moment estimates and focal mechanisms do exist for deep pre-1977 earthquakes (e.g. Wyss, 1970; Sasatani, 1974; Gilbert and Dziewonski, 1975; Chung and Kanamori, 1976; Furumoto and Fukao, 1976). However, because of the variety of methods used (body-wave modeling, mantle-wave modeling, inversion of

normal mode spectra, comer frequency estimates), the resulting datasets remain heterogeneous and fragmentary; in instances when several methods were used on the same event, the results often exhibit considerable scatter. Furthermore, to our knowledge, solutions predating the 1950s are extremely rare, a notable exception being Abe's (1985) study of the Tokai–Oki 1906 earthquake.

Our lack of good estimates on the rates of moment release in the deepest parts of slabs poses a major problem which hinders a better understanding of the processes responsible for seismic failure in deep Wadati–Benioff zones: our quantitative knowledge of deep source parameters (true size, geometry, as well as other features such as time function and stress drop most easily derived from digital datasets) is at present limited, and for practical purposes cannot be taken as extending back more than the 16 years covered by the Harvard CMT dataset. Any further progress in this respect will require an extension of reliable moments for deep earthquakes into the era predating the Harvard CMT catalog. The present paper reports on the preliminary results of this endeavor.

2. Theoretical background: why should it work?

Stated briefly, the CMT algorithm (Dziewonski et al., 1981) consists of the inversion of complete three-component long-period seismograms for the moment tensor and point-source location which maximize the agreement between observed and calculated waveforms. Synthetic seismograms are calculated by summing all the Earth's normal modes up to 45 s period, including path-averaged corrections for the lateral heterogeneity of seismic velocities in the Earth (Dziewonski and Woodward, 1992). In the routine analysis of current global seismicity, seismograms from more than 40 digital stations of the Global Seismic Network are commonly used.

The major problems we face when applying the CMT algorithm to older data result from the nature of the available seismograms: they are usually much scarcer and written on instruments with narrower frequency response than current instruments. For the purpose of the present study, we identify three epochs: (1) we do not consider here events occurring in the years 1972–1976: for these dates, some digital data exist from the high gain long period (HGLP) network. The processing of these data should be straightforward, once reliable information is obtained regarding the instrument responses during this period of development and experimentation of the digital network; it is anticipated that these years will be covered as part of the general CMT project at Harvard. (2) Between 1963 and 1971, generally abundant World Wide Standardized Seismograph Network (WWSSN) data are available on microfilm. (3) Before 1963, no standardized network was available, and datasets with reliable instrument responses can be extremely scarce even for events as late as the mid-1950s; one of the goals of the present study is to explore the feasibility of performing single-station inversions.

The somewhat puzzling suggestion that robust moment tensor solutions can be retrieved from very limited datasets goes back to Buland and Gilbert (1976), who showed that it is theoretically possible to invert a single, non-naturally rotated, horizontal record into the full time history of the moment tensor. Ekström et al. (1986) then demonstrated the practical feasibility of retrieving the static moment tensor from a single three-component broad-band station. Meanwhile, Westaway et al. (1985) showed that WWSSN records can be used to supplement sparse digital datasets. These results suggest that the CMT algorithm is robust, and often yields good results even with limited station coverage, and that, at least for the WWSSN era, analog records are of sufficient quality to be used in the analysis. We wish briefly to discuss here circumstances which suggest that deep earthquakes will be particularly well suited for CMT analysis even when data are scarce, of limited dynamic range, or generally of less than perfect quality.

In simple terms, to be successful a single-station inversion must use a data space of a dimension sufficient to insure that the rank of the resolving matrix be five (note that the standard

Table 1
Centroid coordinates and parameters derived from moment tensor inversions

No.	Centroid parameters												
	Date			Time				Latitude		Longitude		Depth	
	Year	Month	Day	h	min	s	δt_0	λ	$\delta\lambda_0$	ϕ	$\delta\phi_0$	h	δh_0
1	1971	1	29	21	58	9.4 ± 0.3	4.0	51.60 ± 0.02	0.17	151.01 ± 0.05	0.06	524.0 ± 1.9	20.0
2	1969	3	31	19	25	30.2 ± 0.4	3.0	38.46 ± 0.05	0.13	133.83 ± 0.08	−0.77	418.3 ± 2.6	1.3
3	1968	10	7	19	20	28.5 ± 0.2	7.7	26.40 ± 0.02	0.11	140.28 ± 0.03	−0.42	489.9 ± 1.6	−28.1
4	1966	3	17	15	50	38.5 ± 0.3	5.4	-20.98 ± 0.04	0.12	-178.96 ± 0.03	0.24	647.5 ± 2.3	8.5
5	1963	8	15	17	25	31.2 ± 0.2	25.3	-13.41 ± 0.02	0.39	-69.54 ± 0.02	−0.24	571.2 ± 1.5	28.2
6	1962	12	8	21	27	29.3 ± 0.3	7.3	-25.88 ± 0.02	−0.08	-63.35 ± 0.04	0.05	590.3 ± 1.6	−29.7
7	1962	9	29	15	18	15.1 ± 1.8	28.1	-25.13 ± 0.17	1.87	-62.68 ± 0.09	0.92	597.2 ± 3.8	22.2
8	1969	2	10	22	58	11.7 ± 0.5	5.9	-22.93 ± 0.05	−0.22	178.68 ± 0.05	0.07	666.9 ± 3.8	−6.1
9	1969	1	24	2	33	9.6 ± 0.5	6.1	-21.94 ± 0.06	−0.06	-179.58 ± 0.04	0.00	601.8 ± 3.4	6.6
10	1968	11	4	9	7	41.7 ± 0.4	3.2	-14.20 ± 0.04	−0.02	172.14 ± 0.04	0.11	607.0 ± 2.9	22.0
11	1967	3	24	9	0	23.7 ± 0.6	4.6	-6.11 ± 0.05	−0.12	112.17 ± 0.06	−0.16	603.4 ± 5.9	8.4
12	1967	2	15	16	11	18.7 ± 0.4	7.2	-8.76 ± 0.04	0.31	-71.10 ± 0.05	0.28	602.3 ± 2.8	7.3
13	1965	7	6	18	36	48.9 ± 0.5	1.5	-4.65 ± 0.04	−0.15	155.10 ± 0.05	0.00	511.4 ± 4.5	1.4
14	1962	12	7	14	3	45.4 ± 0.3	8.4	28.96 ± 0.03	−0.24	139.52 ± 0.04	0.32	424.5 ± 1.8	13.5
15	1962	9	10	15	44	6.0 ± 0.6	6.6	-20.64 ± 0.07	0.45	-179.12 ± 0.04	0.08	642.4 ± 3.3	2.2
16	1962	5	21	21	15	53.0 ± 0.3	23.0	-19.33 ± 0.04	0.47	-177.37 ± 0.03	0.03	393.5 ± 1.4	51.5
17	1962	3	7	11	1	9.3 ± 0.3	4.7	19.10 ± 0.02	0.10	144.94 ± 0.05	−0.16	661.8 ± 2.6	−23.2
18	1984	3	6	2	17	25.6 ± 1.0	4.6	29.35	FIX	138.92	FIX	455.2 ± 6.3	1.2
19	1957	4	16	4	4	10.6 ± 0.5	1.1	−4.35	FIX	107.30	FIX	635.6 ± 4.4	13.6
20	1922	1	17	3	50	34.3 ± 1.3	−3.6	−3.00	FIX	−70.00	FIX	663.7 ± 8.8	3.7
21	1911	4	28	9	51	57.4 ± 0.9	16.4	−9.50	FIX	−71.20	FIX	556.8 ± 6.5	−5.2

CMT algorithm solves only for the deviatoric part of the source, and thus imposes a zero-trace condition on the moment tensor). To avoid situations where the matrix merely approaches singularity, we must consider a large enough number of normal modes providing significantly independent kernels for the various moment tensor components. In the case of deep earthquakes, the following factors combine to work to our advantage:

(1) The abundant excitation of overtone branches insures a rapid variation of the moment tensor kernels with frequency, even at relatively high frequencies. Hence the possibility of using more narrowly peaked instruments, generally higher frequencies and consequently smaller shocks, as demonstrated by Ekström et al.'s (1986) successful processing of a deep shock of moderate size ($h = 384$ km; $M_0 = 6 \times 10^{26}$ dyn-cm) using single-station Global Digital Seismographic Network (GDSN) data.

(2) The excitation coefficients for the various components of the moment tensor are of comparable amplitude for deep earthquakes—in contrast to the situation with shallow sources for which the $M_{r\theta}$ and $M_{r\phi}$ kernels can be smaller by one order of magnitude, leading to a computational singularity in the inversion process.

(3) The part of the seismograms carrying the most importance in the inversion of deep sources consists of the multiply reflected groups such as PP, PPP, PPS, SSS, etc., a result not surprising as these phases, taken as a whole, represent the mantle overtones whose kernels are crucial to the non-singularity of the resolving matrix. In general, they are the most prominent component of long-period teleseismic records from deep earthquakes, and are not contaminated by fundamental-mode surface waves as is the case for shallow events. The separation of the multiple phases efficiently constrains epicentral distance.

(4) Along similar lines, upgoing energy and downgoing energy from deep earthquakes are well separated in the seismogram, even at rela-

Half drtn	Scale factor 10^{ex}	Principal axes									Best double couple						
		T-Axis			N-Axis			P-Axis			M_0	Plane 1			Plane 2		
		σ	δ	ξ	σ	δ	ξ	σ	δ	ξ		ϕ_s	θ	λ	ϕ_s	θ	λ
5.3	26	1.84	28	131	0.07	16	33	−1.92	57	277	1.9	256	22	−45	28	74	−106
4.3	25	6.29	31	153	1.93	39	33	−8.22	35	268	7.3	298	40	−4	31	88	−130
4.0	26	8.70	10	223	−0.78	31	127	−7.93	57	329	8.3	345	44	−43	108	62	−125
4.9	25	8.71	26	128	−0.21	10	223	−8.5	61	332	8.6	194	21	−120	46	72	−79
16.9	27	3.42	11	302	1.55	21	207	−4.98	66	58	4.2	57	38	−54	194	60	−115
9.0	26	6.06	38	273	−0.07	10	174	−6.14	50	72	6.1	54	12	−30	173	84	−100
4.3	25	6.12	18	258	1.52	8	166	−7.64	70	53	6.9	1	28	−72	162	64	−99
8.0	26	5.09	3	266	0.49	44	173	−5.58	46	359	5.3	31	57	−34	142	62	−141
4.9	25	8.25	36	91	−0.84	20	197	−7.4	47	310	7.8	124	21	−164	19	84	−70
3.9	25	4.54	13	285	1.12	5	193	−5.65	76	82	5.1	22	32	−80	190	58	−96
4.8	25	8.24	22	359	0.57	29	102	−8.81	53	237	8.5	49	34	−148	291	72	−60
6.6	26	3.36	7	263	−0.36	1	353	−2.99	83	93	3.2	352	38	−92	174	52	−88
3.0	25	2.00	27	0	0.20	1	270	−2.20	63	178	2.1	93	18	−87	269	72	−91
5.5	26	1.23	33	72	−0.12	17	174	−1.11	51	286	1.2	114	19	−151	356	81	−73
4.0	25	4.90	3	266	0.66	44	173	−5.55	46	359	5.2	32	57	−34	142	62	−142
14.0	27	2.17	42	103	0.25	5	197	−2.42	48	292	2.3	140	5	−148	17	87	−85
6.9	26	2.53	9	224	0.47	18	131	−3.00	69	339	2.8	335	39	−60	119	57	−112
4.3	27	1.44	42	48	−0.01	13	150	−1.42	45	254	1.4	68	13	−173	331	88	−77
10.5	26	2.07	1	204	1.04	14	113	−3.11	76	297	2.6	307	46	−70	100	48	−109
9.4	27	7.86	20	287	−1.62	17	191	−6.24	63	63	7.1	44	30	−53	183	67	−109
9.4	26	4.06	11	94	−0.74	0	4	−3.32	79	273	3.7	184	34	−90	4	56	−90

tively long periods, and their relative phase shift is easily resolved in the inversion to provide centroid depth.

(5) Deep earthquakes most commonly have shorter durations than shallow ones of similar moment (Vidale and Houston, 1993), justifying our assumption of a point source and of a box-car source rate time function with a duration given by scaling arguments, for all but the largest deep events.

On the other hand, the specific limitations introduced by applying the CMT algorithm to historical single-station and limited datasets must also be assessed:

(1) a possible limitation of the technique of single-station inversion, pointed out by Ekström et al. (1986), is that it cannot resolve the location of the centroid in a direction perpendicular to the great circle involved. In the present study, this is only a minor inconvenience: most of the earthquakes considered will be of such magnitude as to allow, if necessary, a relocation based on published International Seismological Centre (ISC) travel times. Although any significant difference between centroid and hypocenter locations is in itself interesting, the focus of our study is the focal mechanism and seismic moment of the seismic source. In practice, the inversions can be carried out with constrained epicenters to stabilize the inversion. If the epicenter is fixed, but misplaced, the focal solution inverted from a single-station dataset is not always robust. However, the quality of the solution, as represented by its variance reduction, is optimized at the true epicenter. This property can be used to refine the choice of the fixed epicenter.

(2) A potentially more important limitation stems from our limited knowledge of instrument responses; both amplitude and, equally important, phase responses must be reliably known in the period range 35–80 s, to obtain accurate CMT solutions. In this respect, and as discussed in more detail below, we will emphasize instrument–station combinations for which full and reliable documentation of instrument characteristics is available.

Table 2
Elements of the moment tensor obtained in the CMT inversions

No.	Scale 10^{ex}	M_{rr}	$M_{\theta\theta}$	$M_{\phi\phi}$	$M_{r\theta}$	$M_{r\phi}$	$M_{\theta\phi}$
1	26	-0.96 ± 0.04	0.67 ± 0.06	0.29 ± 0.06	-0.59 ± 0.05	-1.44 ± 0.06	0.62 ± 0.05
2	25	-0.26 ± 0.22	4.45 ± 0.37	-4.18 ± 0.40	-1.52 ± 0.38	-5.65 ± 0.35	1.59 ± 0.33
3	26	-5.56 ± 0.15	2.64 ± 0.24	2.91 ± 0.28	-3.98 ± 0.22	-0.56 ± 0.21	-5.50 ± 0.25
4	25	-4.83 ± 0.19	0.97 ± 0.25	3.86 ± 0.25	-5.24 ± 0.24	4.46 ± 0.23	2.66 ± 0.25
5	27	-3.80 ± 0.09	1.74 ± 0.11	2.06 ± 0.12	-1.10 ± 0.12	2.38 ± 0.11	1.30 ± 0.12
6	26	-1.27 ± 0.10	-0.17 ± 0.11	1.44 ± 0.14	-0.82 ± 0.14	5.82 ± 0.13	0.92 ± 0.13
7	25	-6.09 ± 0.39	1.29 ± 0.40	4.81 ± 0.53	-2.07 ± 0.44	3.70 ± 0.43	-0.29 ± 0.45
8	26	-2.66 ± 0.19	-2.39 ± 0.22	5.05 ± 0.22	-3.05 ± 0.22	0.21 ± 0.22	-0.40 ± 0.24
9	25	-1.18 ± 0.26	-2.09 ± 0.41	3.27 ± 0.31	-2.17 ± 0.30	-6.84 ± 0.32	-1.4 ± 0.32
10	25	-5.06 ± 0.20	1.32 ± 0.29	3.75 ± 0.31	-0.02 ± 0.22	2.34 ± 0.34	0.85 ± 0.29
11	25	-4.33 ± 0.44	6.20 ± 0.56	-1.87 ± 0.57	5.07 ± 0.55	-3.76 ± 0.60	1.68 ± 0.65
12	26	-2.89 ± 0.11	-0.31 ± 0.18	3.20 ± 0.23	-0.04 ± 0.13	0.81 ± 0.15	-0.43 ± 0.13
13	25	-1.31 ± 0.08	1.11 ± 0.17	0.20 ± 0.18	1.71 ± 0.15	0.04 ± 0.15	-0.02 ± 0.13
14	26	-0.32 ± 0.02	-0.05 ± 0.03	0.37 ± 0.03	0.06 ± 0.03	-1.05 ± 0.03	-0.38 ± 0.03
15	25	-2.51 ± 0.17	-2.35 ± 0.23	4.86 ± 0.17	-3.12 ± 0.25	0.17 ± 0.24	-0.38 ± 0.20
16	27	-0.36 ± 0.04	0.13 ± 0.08	0.22 ± 0.07	-0.72 ± 0.05	-2.16 ± 0.05	-0.19 ± 0.06
17	26	-2.51 ± 0.07	1.12 ± 0.08	1.40 ± 0.12	-1.31 ± 0.09	-0.18 ± 0.10	-1.15 ± 0.09
18	27	-0.07 ± 0.16	0.28 ± 0.16	-0.21 ± 0.06	0.67 ± 0.08	-1.22 ± 0.10	-0.21 ± 0.21
19	26	-2.86 ± 0.43	1.85 ± 0.32	1.01 ± 0.17	-0.47 ± 0.18	-0.87 ± 0.15	-0.48 ± 0.56
20	27	-4.24 ± 1.84	-1.07 ± 0.74	5.31 ± 2.36	0.04 ± 0.79	4.51 ± 0.63	2.77 ± 2.52
21	26	-3.05 ± 0.90	-0.72 ± 0.32	3.77 ± 1.05	-0.09 ± 0.34	-1.38 ± 0.29	0.33 ± 1.06

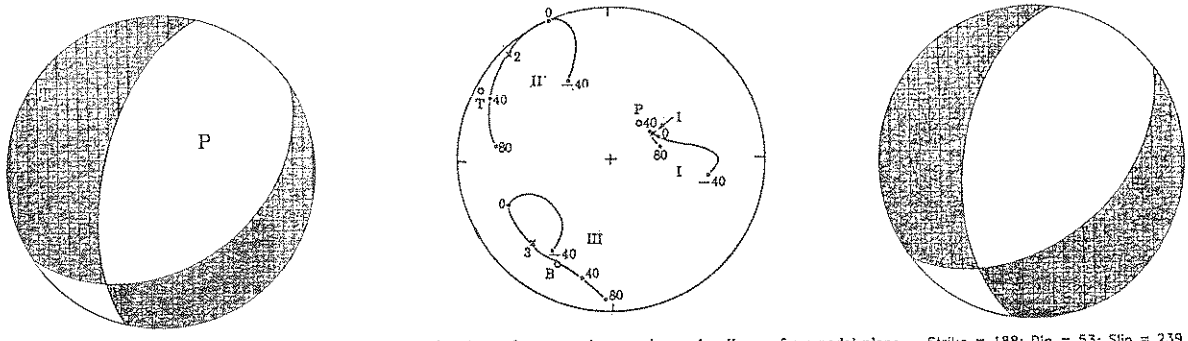

Strike = 194; Dip = 60; Slip = 245

o, P, T, B: directions of compression, tension and null axes from nodal plane solutions; ×, I, II, III: directions of principal axes of the moment tensor

Strike = 188; Dip = 53; Slip = 239

Eigenvalues and eigenvectors of the deviatoric moment tensor

Index i	This study			Gilbert and Dziewonski (1975)		
	Eigenvalue D_i (10^{27} dyn-cm)	Plunge η_i (deg)	Azimuth ζ_i (deg)	Eigenvalue D_i (10^{27} dyn-cm)	Plunge η_i (deg)	Azimuth ζ_i (deg)
1	−5.0	66	58	−4.0	63	68
2	1.6	22	207	1.3	26	225
3	3.4	11	302	2.7	6	318

Fig. 1. Results of the CMT inversion of the 15 August 1963 Peru–Brazil earthquake (left) compared with Gilbert and Dziewonski's (1975) inversion using an extensive dataset (center) and with Chandra's (1970) first motion mechanism (right). In the center diagram, the solid lines represent the loci of the principal axes of the mechanism projected on the lower focal hemisphere, as they varied with time during the evolution of the source, as derived by the researchers. We also compare the eigenvectors of our best-fitting deviatoric moment tensor (including the minor double-couple) with those of Gilbert and Dziewonski, given by their amplitudes D, plunges η and azimuths ζ. The excellent overall agreement is noteworthy.

In summary, initial considerations indicate why deep earthquakes should be well suited for analysis using the CMT technique. The primary source of uncertainty is likely to stem from incomplete knowledge of the response characteristics of the seismograph.

3. Datasets

We used the body-wave portion of the seismograms to perform the inversions. Records were digitized over a window starting at the origin time of the event, and ending at a group time corresponding to 4.4 km s^{-1}—the expected arrival time of the first passage of the Love waves. To guard against instrumental instabilities, which can be very prominent on horizontal WWSSN records, we used only seismograms with high long-period signal-to-noise ratio. Stations at epicentral distances shorter than 30° were not used. Results are summarized in Tables 1 and 2. Their format is that of the quarterly reports of Dziewonski et al. in Physics of the Earth and Planetary Interiors, with two minor exceptions: the addition of the year of the event in Column 2, and the occasional entry 'FIX' in the epicentral columns, indicating that the inversion was carried out with a constrained epicenter. For a full explanation of the headings, readers are referred to Dziewonski et al. (1987).

3.1. WWSSN events

Our primary goals for events between 1962 and 1971 were (1) to test the inversion algorithm on a small number of well-studied events, (2) to assess the quality of moments available in the literature, (3) to investigate the minimum number of stations and records necessary to obtain a robust solution. With these multiple goals in mind, we selected 17 earthquakes, seven of which had

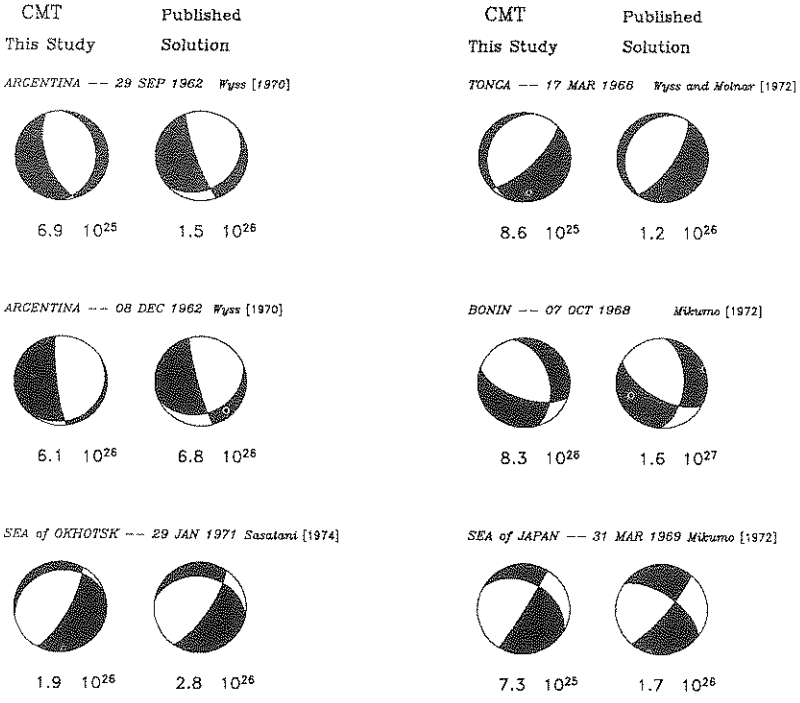

Fig. 2. CMT solutions obtained from WWSSN records for six events whose moment is available from previous studies, compared with the published solutions. The values of the scalar moment (in dyn cm) are also compared. When several values resulting from different methods were reported, the published value represents their geometrical average.

focal solutions and moment values published in the literature (Events 1–7 in Table 1, sorted by increasing age).

Fig. 1 gives the example of the great Peru–Bolivia earthquake of 15 August 1963 (Event 5). Both the geometry of our solution and the moment obtained using 10 stations compare favorably with the results of the extensive study by Gilbert and Dziewonski (1975), who used mostly single-component (Z) records of up to 20 h duration at 37 stations. In particular, not only do we reproduce the best double-couple geometry (also in excellent agreement with Chandra's (1970) first motion solution), but we also fit the secondary

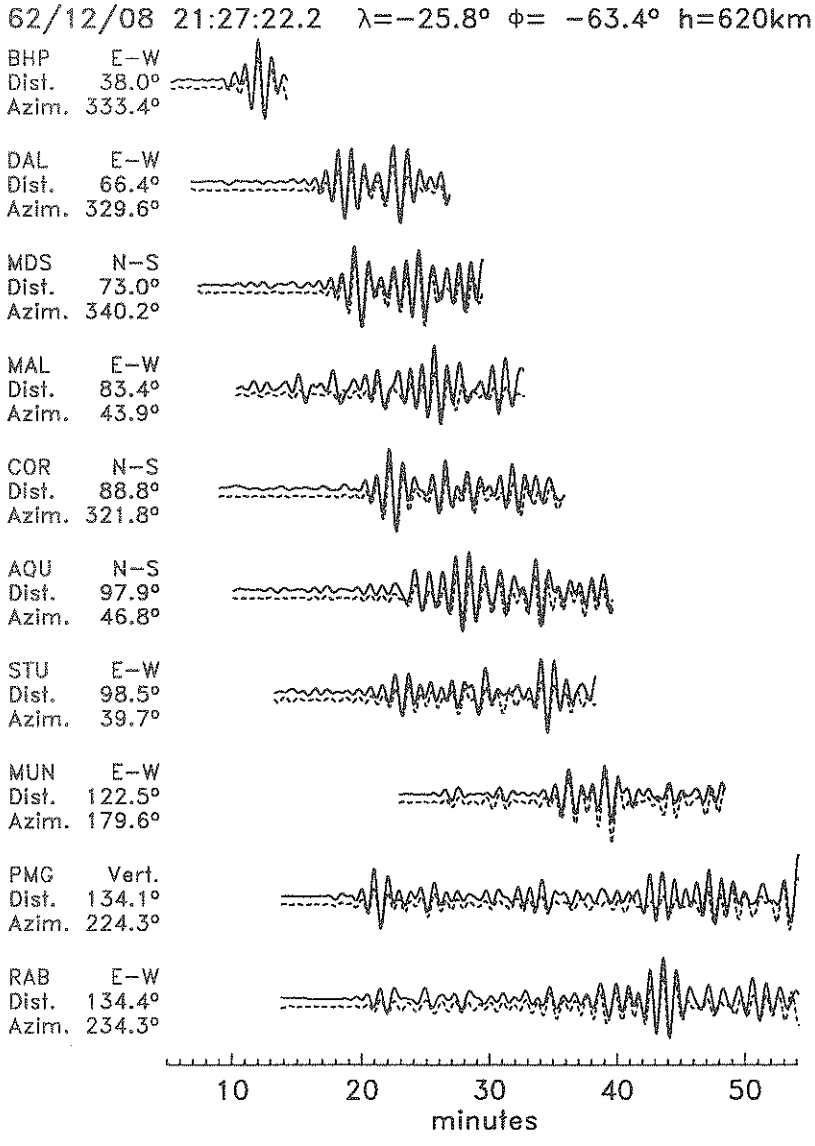

Fig. 3. Comparison of observed and synthetic seismograms in the case of Event 6. For each station a representative component has been selected. The top (full) traces are the filtered WWSSN seismogram windows used in the inversion; the bottom (dashed) ones are the synthetic seismograms computed for the inverted CMT solution. This figure is directly comparable with such plots for modern events as Fig. 4 of Dziewonski and Woodhouse (1983).

double-couple, as documented by the table at the bottom of Fig. 1. Although this result is not surprising, given that the CMT algorithm derives directly from Gilbert and Dziewonski's (1975) formalism, it is nevertheless important, in view of the much reduced size of our dataset.

Fig. 2 illustrates the case of smaller events, for which moments were published by various workers. In general, the focal mechanisms are reproduced remarkably well. The moment values are also in good agreement, especially given the large scatter occasionally reported by these workers, when several techniques (body waves, surface waves) were used. Fig. 3 shows the fit between observed seismograms and synthetic ones computed for the final solution, in the case of the 1962 deep earthquake in Argentina (Event 6). The fit compares favorably with that for modern CMT events, as documented for example in Fig. 4 of Dziewonski and Woodhouse (1983).

We also show in Fig. 4 a compilation of an additional 10 events (Events 8–17 in Table 1, ordered by increasing age) for which a first motion focal mechanism, but to our knowledge no moment value, is available in the literature. Our results are in generally excellent agreement with the published geometries, with two exceptions. In the case of Event 14 (7 December 1962), our solution requires less strike-slip than the mechanism published by Wickens and Hodgson (1967) (and compiled by Denham (1977)) but the two solutions have T-axes only 22° apart and they share a common fault plane. In the case of Event 8, the mechanism in disagreement, listed by Denham (1977), is unpublished in the literature.

We further investigated to which extent the

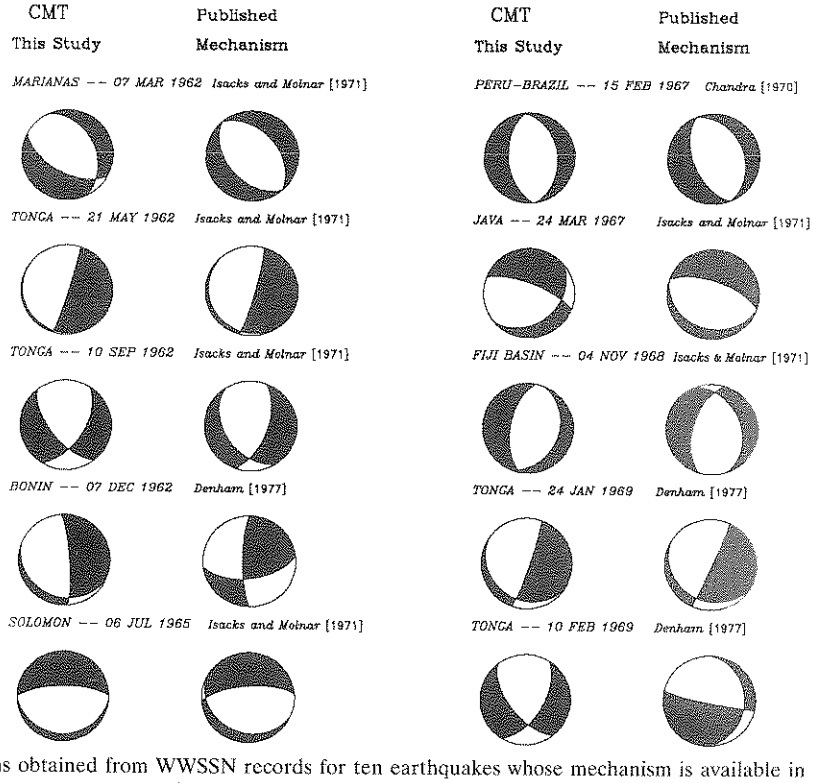

Fig. 4. CMT solutions obtained from WWSSN records for ten earthquakes whose mechanism is available in the literature, but for which no moment could be compiled. (Note the generally excellent agreement in geometry.) The 10 February 1969 mechanism listed by Denham (1977) is unpublished in the literature.

solution is degraded when the number of stations used is reduced. For this purpose, we used Event 1, and carried out inversions for all 15 possible combinations of (one to four among) the digitized stations. As documented in Fig. 5, the results show remarkable robustness: the deviation of the solutions from the preferred one (obtained from the full four-station dataset), as measured by the angular distance of the relevant principal axes, does not exceed 20°, and the moment varies by at most 37%, or 0.09 units of M_w. Furthermore, the depths obtained in the inversions are all within 10 km of the four-station centroid depth. On the other hand, we found that two-station inversions could result in an epicenter mislocated by as much as 2.5°. One-station inversions could not resolve the centroid, and had to be carried out with fixed epicenter. The conclusion of this experiment is that a dataset of three stations gives excellent CMT solutions; so does even a single-station inversion, but at the cost of constraining the epicenter.

3.2. Earlier events

Regarding pre-WWSSN events, the major problem is that of acquiring data from instruments with documented, reliable responses. One such system is the three-component Press–Ewing seismometer operated at Pasadena since the mid-1950s and discontinued in 1992 (H. Kanamori, personal communication, 1993). Before analyzing any historical earthquake, we elected to test the reliability of this instrument in single-station inversions, by processing a single three-component record at Pasadena for a few recent events for which a CMT solution is available. We further explored the possibility of using only two horizontal components, a typical situation with historical records. Fig. 6 compares the result of our inversion of the 6 March 1984 earthquake (Event 18 in Table 1) with the published CMT solution. The agreement is outstanding.

We then proceeded to invert a target event, namely the 16 April 1957 deep Java earthquake (Event 19 in Table 1). This earthquake is important as it marks the westernmost limit of deep seismic activity in Java, and has been given a magnitude as high as 7.5 by B. Gutenberg (Rothé, 1969), roughly one unit of magnitude above any recent (post-1963) event (Okal and Kirby, 1993). We conducted a two-component (Z and north-south) single-station inversion (at that time, the east–west component of the Pasadena Press–Ewing instrument was not operating), the results

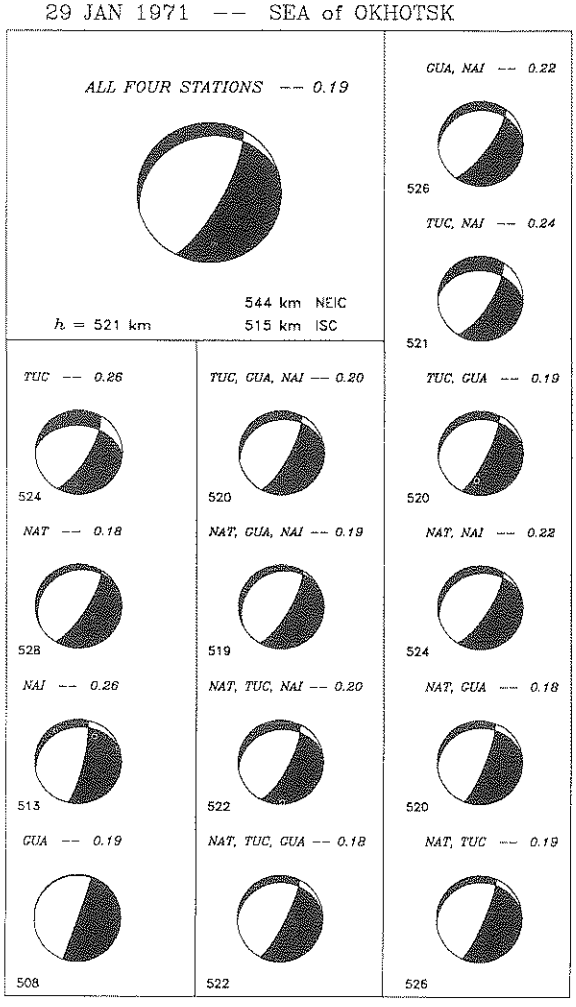

Fig. 5. Experiment designed to assess the minimum number of stations necessary for a reliable CMT solution (Event 1). Each beachball is the result of an inversion carried out with a dataset consisting of the stations listed above it. The inverted moment is listed (in italics in units of 10^{27} dyn-cm) next to the stations, and the inverted depth (in km) at the bottom left. For reference, the ISC and National Earthquake Information Center (NEIC) depths are also given. One-station inversions were carried out with constrained epicenter.

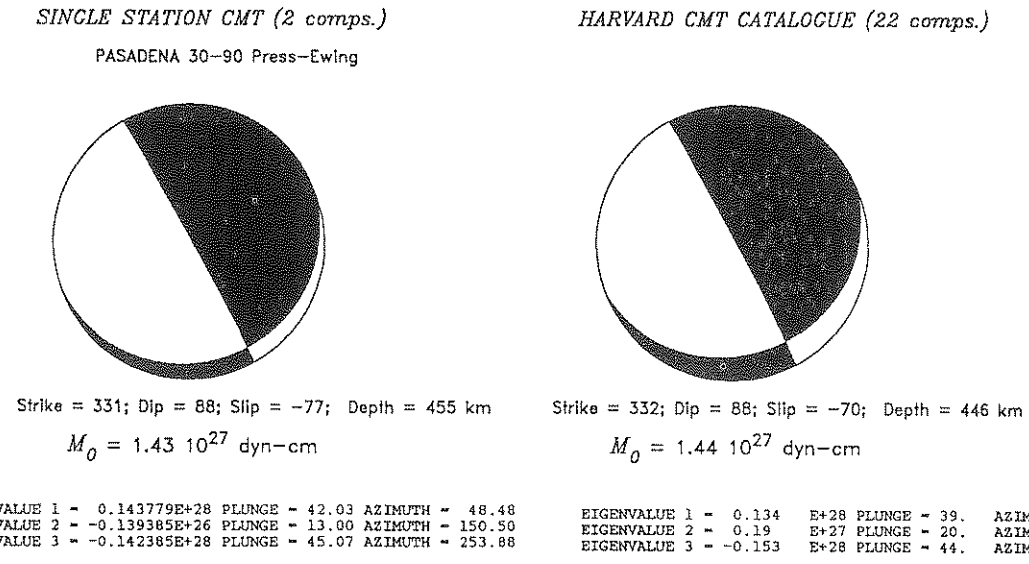

Fig. 6. CMT solution obtained for the 6 March 1984 deep event south of Honshu using only two horizontal Press–Ewing seismograms at Pasadena (left), compared with solution published in the Harvard CMT catalog (right). (Note the outstanding agreement despite the considerably smaller dataset.)

of which are shown in Fig. 7. This study establishes the 1957 earthquake as one of the largest deep earthquakes in Indonesia. It is significantly larger than the only available digital deep CMT solution under West Java. However, comparable (or even larger) earthquakes are documented in the Flores and Banda Seas and the 1957 event does not appear exceptional in this respect.

We proceeded to further testing of the potential for single-station inversions of Wiechert and Galitzin seismograms, given the large numbers of these instruments deployed at the beginning of

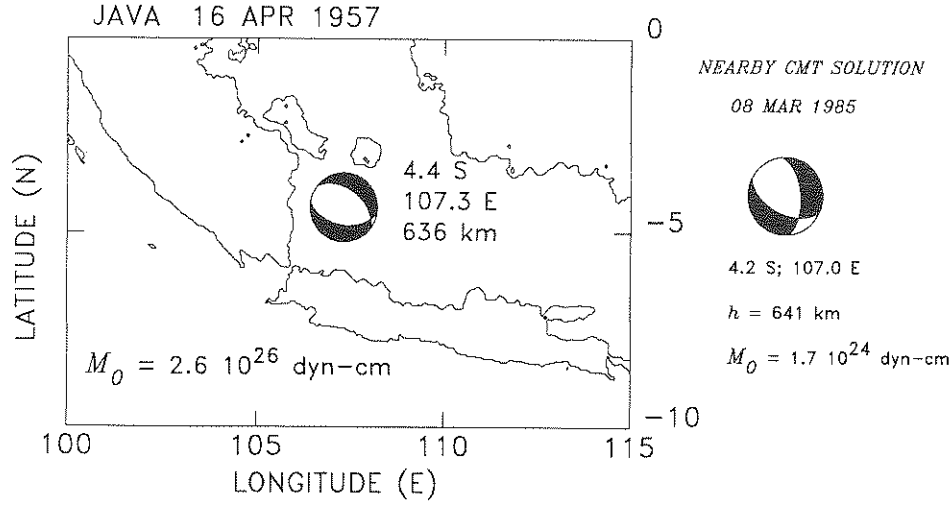

Fig. 7. Map and inverted geometry of the 1957 deep Indonesian earthquake. Also shown is the only CMT solution available for deep events below west Java.

the century. We selected for inversion the Uppsala Wiechert records of the 1922 deep Peruvian earthquake (Event 20 in Table 1; (Okal and Bina, 1994)). The inversion must be carried out at fixed epicenter, and converges acceptably only for a distance of about 91.5°, which requires moving the epicenter slightly to the NE. The resulting focal solution (see Fig. 8) has a downdip compressional axis. It shares its character of vertical compression with the nearby (and significantly larger) 1970 deep Colombian event, with the P axes of the two earthquakes only 16° away from each other.

Finally, the earliest event we investigated is the South American earthquake of 28 April 1911 (Event 21), for which we processed a two-component horizontal Galitzin seismogram from Pulkovo, Russia, obtained in the microfilmed archives of the US Geological Survey at Denver (Glover and Meyers, 1987), with detailed instrument calibration available on the microfilm. This event is of interest as its original location is at 0°N, 71°W, in the vicinity of the 1970 Colombian shock (Gutenberg and Richter, 1954); however, we relocated it to the Peru–Brazil subduction segment (Okal and Bina, 1994). The CMT solution could not converge satisfactorily for the original epicenter (8° closer to Pulkovo), and its focal geometry and moment are comparable with those of nearby present-day CMT solutions (Fig. 9).

4. Conclusion and perspective

We have shown that it is feasible to apply the CMT technique to deep earthquakes, predating the deployment of the digital seismic network. Our tests have shown that (1) we can reproduce existing moment tensor solutions from small datasets of WWSSN records (in practice as few as

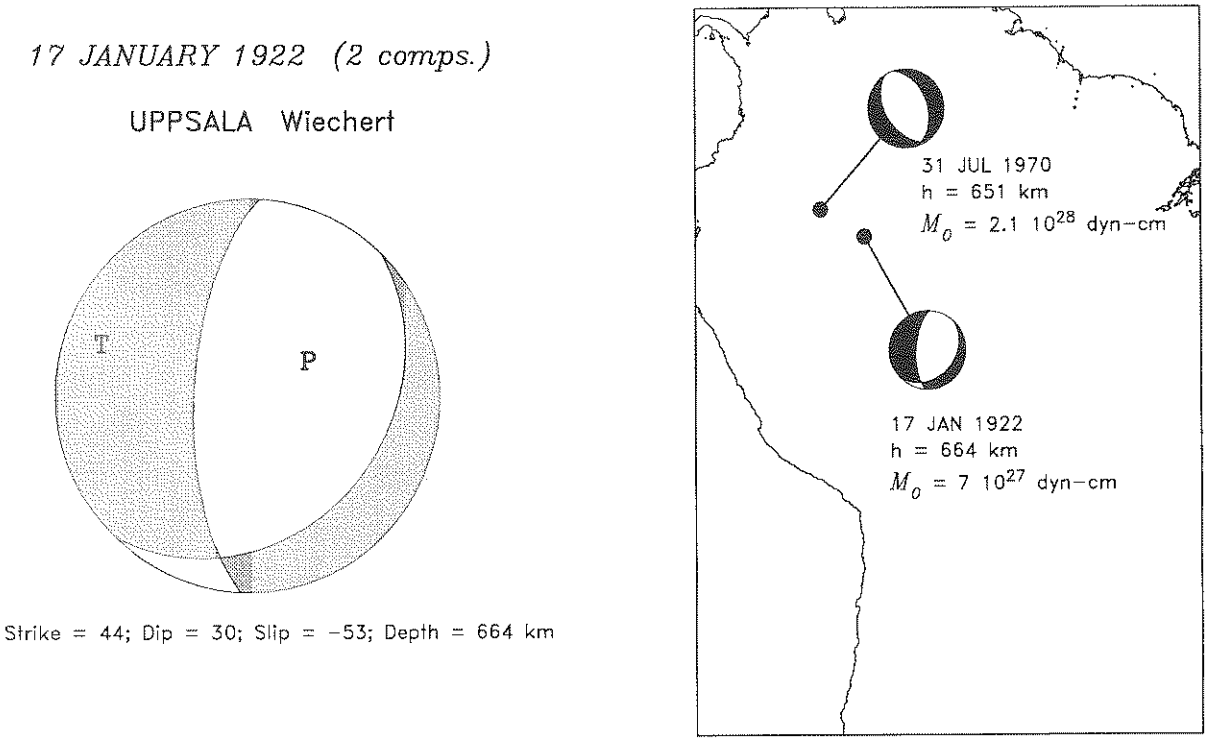

Fig. 8. CMT solution inverted from the Uppsala Wiechert horizontal records for the deep earthquake of 17 January 1922 in northern Peru. The inversion was carried out with constrained epicenter. Map shows spatial relationship to the 1970 deep Colombian shock, and compares their mechanisms.

three stations), (2) robust moment tensor solutions can be obtained from single-station datasets by constraining the epicenter, and (3) pre-WWSSN records can be used to retrieve CMT solutions for historical events, as long as reliable documentation of instrumental characteristics is available. This is particularly crucial for electromagnetic seismographs, for which the values of the components of the electrical circuits have occasionally been adjusted without precise documentation, especially during the development stages of the instruments. In particular, our experience has been that many Press–Ewing instruments deployed during the International Geophysical Year (1957–1958) reflect this problem. On the other hand, the mechanical instruments, and notably the Wiechert seismometers deployed in large numbers around the turn of the century, should be expected to have undergone fewer adjustments. In all cases, and given the intrinsic power of the method with datasets of as few as one station, it is highly preferable to emphasize well-documented instruments, rather than to add a station with a questionable response. We also

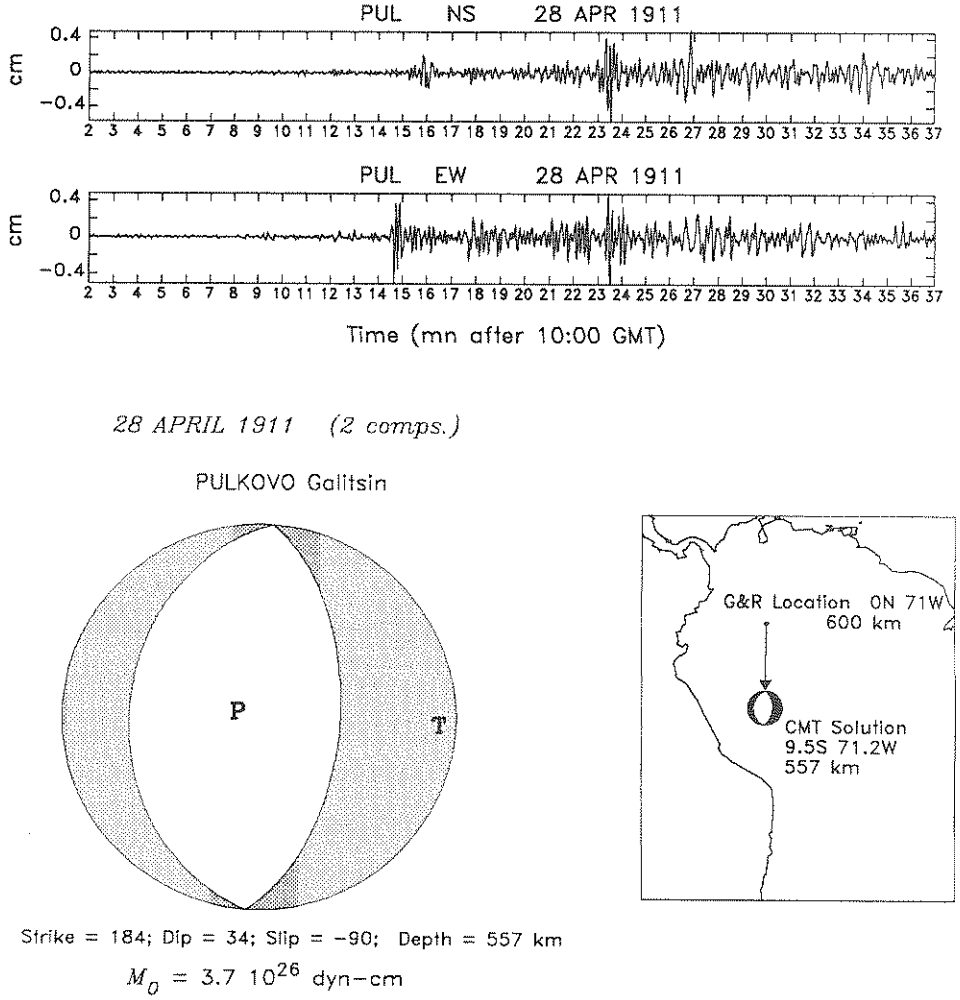

Fig. 9. Inversion of the deep 1911 Peru–Brazil event. Top: digitized Pulkovo seismograms. The traces start at 10:02 h GMT, i.e. approximately 10 min after origin time. Bottom left: inverted CMT solution (Note down-dip compressional character.) Bottom right: map of the relocation vector for the event, obtained from a combination of Okal and Bina (1994) and the present study.

note that the matching of a complete waveform provides a constraint on the epicentral distance which is insensitive to the quality of timing at the station.

The stage is then set for a systematic effort aimed at extending the CMT catalog for deep events ($h \geq 300$ km), as far back in time as the 1910s and possibly the turn of the century, when networks of Wiechert and Galitzin instruments were deployed. This endeavor should provide significant additional insight into the characteristics of deep seismicity. We would expect to be able to add more than 100 deep events with $M_0 \geq 10^{25}$ dyn-cm to the existing CMT catalog, at least a two-third increase over the currently available dataset. As of the time of writing (13 February 1994), we have computed over 60 preliminary solutions based on WWSSN data and covering the years 1964–1971, and are preparing a catalog of these CMT solutions in the exact format of the Harvard catalog for modern events, including in particular all five deviatoric moment components and an estimate of their uncertainties (Huang et al., 1994).

Acknowledgments

We are grateful to Hiroo Kanamori and Ines Cifuentes for detailed information on instrument responses. Ota Kulhánek made available to E.A.O. the superb archives at Uppsala, from which the 1922 Peruvian records were extracted, and provided facilities for digitizing the original records. We benefited from many hours of discussion with Steve Kirby on the matter of deep slab processes. This research has been supported by grants EAR-92-19361 and EAR-93-16396 from the National Science Foundation.

References

Abe, K., 1985. Re-evaluation of the large deep earthquake of January 21, 1906. Phys. Earth Planet. Inter., 39: 157–166.

Buland, R.P. and Gilbert, F., 1976. Matched filtering for the seismic moment tensor. Geophys. Res. Lett., 3: 205–206.

Burnley, P.C. and Kirby, S.H., 1982. Pressure-induced embrittlement of polycrystalline tremolite (abstract). Eos, Trans. Am. Geophys. Union., 63: 1095.

Burnley, P.C., Green, H.W. and Prior, D., 1991. Faulting associated with the olivine-to-spinel transformation in Mg_2GeO_4 and its implications for deep-focus earthquakes. J. Geophys. Res., 96: 425–443.

Chandra, U., 1970. The Peru–Bolivia border earthquake of August 15, 1963. Bull. Seismol. Soc. Am., 60: 639–646.

Chung, W.-Y. and Kanamori, H., 1976. Source process and tectonic implications of the Spanish deep-focus earthquake of March 29, 1954. Phys. Earth Planet. Inter., 13: 85–96.

Creager, K.C. and Jordan, T.H., 1984. Slab penetration into the lower mantle. J. Geophys. Res., 89: 3031–3049.

Denham, D., 1977. Summary of earthquake focal mechanisms for the Western Pacific–Indonesian region, 1929–1973. US Dept. Commerce, World Data Center A, Boulder, Rep. SE-3, 110 pp.

Dziewonski, A.M. and Woodhouse, J.H., 1983. An experiment in systematic study of global seismicity: centroid moment tensor solutions for 201 moderate and large earthquakes of 1981. J. Geophys. Res., 88: 3247–3271.

Dziewonski, A.M. and Woodward, R.L., 1992. Acoustic imaging at the planetary scale. In: H. Emert and H.-P. Harjes (Editors), Acoustical Imaging, Vol. 19. Plenum, New York, pp. 785–797.

Dziewonski, A.M., Chou, T. and Woodhouse, J.H., 1981. Determination of earthquake source parameters from waveform data for studies of global and regional seismicity. J. Geophys. Res., 86: 2825–2852.

Dziewonski, A.M., Friedman, A., Giardini, D. and Woodhouse, J.H., 1983. Global seismicity of 1982: centroid moment tensor solutions for 308 earthquakes. Phys. Earth Planet. Inter., 33: 76–90.

Dziewonski, A.M., Ekström, G., Franzen, J.E. and Woodhouse, J.H., 1987. Global seismicity of 1977: centroid moment tensor solutions for 471 earthquakes. Phys. Earth Planet. Inter., 45: 11–36.

Ekström, G., Dziewonski, A.M. and Stein, J.M., 1986. Single station CMT: application to the Michoacan, Mexico earthquake of September 19, 1985. Geophys. Res. Lett., 13: 173–176.

Furumoto, M. and Fukao, Y., 1976. Seismic moments of great deep shocks. Phys. Earth Planet. Inter., 11: 352–357.

Gilbert, F. and Dziewonski, A.M., 1975. An application of normal mode theory to the retrieval of structural parameters and source mechanisms from seismic spectra. Philos. Trans. R. Soc. London, Ser. A, 278: 187–269.

Glover, D.P. and Meyers, H., 1987. Historical seismogram filming project: current status. In: W.H.K. Lee, H. Meyers and K. Shimazaki (Editors), Historical Seismograms and Earthquakes of the World. Academic Press, London, pp. 373–379.

Griggs, D., 1972. The sinking of the lithosphere and the focal mechanism of deep earthquakes. In: E.C. Robertson (Editor), The Nature of the Solid Earth. McGraw-Hill, New York, pp. 361–384.

Gutenberg, B. and Richter, C.F., 1954. Seismicity of the Earth. Princeton, NJ: Princeton University Press, 310 pp.

Hobbs, B.E. and Ord, A., 1988. Plastic instabilities: implications for the origin of intermediate- and deep-focus earthquakes. J. Geophys. Res., 93: 10521–10540.

Huang, W.-C., Okal, E.A., Ekström, G. and Salganik, M.P., 1994. CMT inversion of analog seismograms of deep earthquakes: progress report on the WWSSN era (abstract). Seismol. Res. Lett., 65: 65.

Isacks, B.L. and Molnar, P., 1971. Distribution of stresses in the descending lithosphere from a global survey of focal-mechanism solutions of mantle earthquakes. Rev. Geophys. Space Phys., 9: 103–174.

Kirby, S.H., Durham, W.B. and Stern, L.A., 1991. Mantle phase changes and deep-earthquake faulting in subducting lithosphere. Science, 252: 216–225.

Lomnitz-Adler, J., 1990. Are deep focus earthquakes caused by a martensitic transformation? J. Phys. Earth, 38: 83–98.

Lundgren, P.R. and Giardini, D., 1992. Seismicity, shear failure and mode of deformation in deep subduction zones. Phys. Earth Planet. Inter., 74: 63–74.

Meade, C. and Jeanloz, R., 1989. Acoustic emissions and shear instabilities during phase transformations in Si and Ge at ultra-high pressure. Nature, 339: 616–618.

Meade, C. and Jeanloz, R., 1991. Deep-focus earthquakes and recycling of water into the Earth's mantle. Science, 252: 68–72.

Mikumo, T., 1972. Focal processes of deep and intermediate earthquakes around Japan as inferred from long-period *P* and *S* waveforms. Phys. Earth Planet. Inter., 6: 293–299.

Molnar, P., Freedman, D. and Shih, J.S.F., 1979. Lengths of intermediate and deep seismic zones and temperatures in downgoing slabs of lithosphere. Geophys. J. R. Astron. Soc., 56: 41–54.

Okal, E.A. and Bina, C.R., 1994. The deep earthquakes of 1921–1922 in Northern Peru. Phys. Earth Planet. Inter., submitted.

Okal, E.A. and Kirby, S.H., 1993. Quantitative reassessment of the intermediate and deep seismicity of the Indonesian arc: preliminary results (abstract). Seismol. Res. Lett., 64: 14.

Raleigh, C.B., 1967. Tectonic implications of serpentinite weakening. Geophys. J. R. Astron. Soc., 14: 113–118.

Rothé, J.-P., 1969. The seismicity of the Earth/La séismicité du globe 1953–1965. UNESCO, Paris, 336 pp.

Sasatani, T., 1974. Source process of a deep-focus earthquake in the Sea of Okhotsk as deduced from long-period *P* and *SH* waves. J. Phys. Earth, 22: 279–297.

Spakman, W., Stein, S., van der Hilst, R. and Wortel, M.J.R., 1989. Resolution experiments for Northwest-Pacific subduction zone tomography. Geophys. Res. Lett., 16: 1097–1100.

Vidale, J.E. and Houston, H., 1993. The duration of deep earthquakes. Nature, 365: 45–47.

Westaway, R.W.S., Ekström, G. and Woodhouse, J.H., 1985. Use of analog WWSSN seismograms in centroid-moment tensor inversion (abstract). Eos, Trans. Am. Geophys. Union, 66: 312.

Wickens, A.J. and Hodgson, J.H., 1967. Computer re-evaluation of earthquake mechanism solutions, 1922–1962. Dept. Energy, Mines & Resources, Ottawa, Publ. Dominion Obs. Ottawa, XXXIII (1), 560 pp.

Wortel, M.J.R., 1986. Deep earthquakes and the thermal assimilation of subducting lithosphere. Geophys. Res. Lett., 13: 34–37.

Wyss, M., 1970. Stress estimates for South American shallow and deep earthquakes. J. Geophys. Res., 78: 1529–1544.

Wyss, M. and Molnar, P., 1972. Source parameters of intermediate and deep focus earthquakes in the Tonga arc. Phys. Earth Planet. Inter., 6: 279–292.

Zhou, H.-W., 1990. Mapping of *P*-wave slab anomalies beneath the Tonga, Kermadec and New Hebrides arcs. Phys. Earth Planet. Inter., 61: 199–229.